APPLICATION OF THE FINITE VOLUME METHOD TO THE RADIAL CONDUCTION MODEL OF THE CATHENA CODE

HYOUNG TAE KIM, BO WOOK RHEE, and BYUNG-JOO MIN

Korea Atomic Energy Research Institute
150 Dukjin-Dong, Yusong-Gu, Daejeon 305-353, Korea
Phone: +82-42-868-8720, Fax: +82-42-868-8256, E-mail: kht@kaeri.re.kr

ABSTRACT

The CATHENA code uses the finite element method (FEM) for the radial conduction model, which determines the temperature distribution from the fuel center to the cladding in the radial direction. However, it has been shown that the finite element solutions in the heat source region such as a fuel pellet are converged to the exact solutions with an increasing number of mesh elements. Since the finite volume method (FVM) ensures local and global energy conservation due to the integral conservation over each control volume, the FVM is applied to CATHENA wall conduction model to avoid the mesh size effect on the fuel temperature prediction.

The accuracy and validity of the finite volume model in the CATHENA code are tested against two cases, a steady state case and a transient heat conduction case, for which exact solutions are available. A constant temperature on the boundary surface and a uniform internal heat generation rate are assumed for the steady state problem. In the transient heat conduction problem, a cylinder is initially at a uniform temperature and suddenly; its boundary surface is subjected to a convection with a constant heat transfer coefficient into an ambient at a constant temperature.

The steady state solutions by the FVM model are found to give the same results as the analytical solutions and consistent results with varying mesh sizes, while the original CATHENA with the FEM over-predicts the center temperature with larger mesh sizes. For the transient problem the FVM model also closely follows the analytic solutions of the dimensionless heat conduction equation for a long cylinder.

1. INTRODUCTION

The finite element method (FEM) [1] has been applied to the solution of a wide range of heat conduction and fluid flow problems. For the CATHENA [2], a thermal-hydraulic analysis code for the CANDU (CANada Deuterium Uranium) reactor, the one-dimensional heat conduction equation is solved subject to the boundary conditions by a FEM, a variational technique in the radial direction of the cylindrical geometry. Since typical cylindrical geometries are fuel pins and tube walls, the CATHENA wall conduction model is important for the prediction of the temperature distribution within the fuel pins.

However, the FEM model in the CATHENA does not necessarily satisfy the physical conservation laws in the form of the differential equations. Therefore, if the one dimensional heat conduction equation is solved for the cylindrical or the spherical geometry, its solutions by the FEM converge to the exact solutions with a sufficient number of elements. For the assessment of the FEM for radial heat conduction in the cylindrical geometry, the FEM solutions for the temperatures at each radial node are compared with the exact solutions.

It is known [3] that even with a coarse grid the finite volume solution of simple diffusion problems involving conductive heat transfer agrees very well with the exact solution, since the finite volume method (FVM) ensures local and global energy conservation due to the integral conservation over each control volume. Therefore, the FVM is applied to the CATHENA wall conduction model to avoid the mesh size effect on the fuel temperature prediction. For this purpose the numerical scheme for the CATHENA radial conduction model is developed and implemented in the CATHENA code.

The accuracy and validity of the finite volume model in the CATHENA code are tested by one-dimensional steady state and transient heat conduction problems in the cylindrical geometry, for which the exact solutions are available. A constant temperature on the boundary surface and a uniform internal heat generation rate are assumed for the steady state problem. In the transient heat conduction problem, a cylinder is initially at a uniform temperature and suddenly; its boundary surface is subjected to convection with a constant heat transfer coefficient into an ambient at a constant temperature.

2. ASSESSMENT OF FEM SOLUTION FOR RADIAL HEAT CONDUCTION

Consider a long solid cylinder of radius R_o in which the energy is generated at a constant rate q_o (W m^{-3}) and a constant thermal conductivity k (W m^{-1}K^{-1}) as shown in Figure 1. The boundary surface at $r = R_o$ is maintained at a constant temperature T_b, and the flux is zero at $r = 0$. Then we are to calculate the temperature distribution $T(r)$.

The governing equation for this problem is as follow:

$$-\frac{1}{r}\frac{d}{dr}\left(2\pi k r\frac{dT}{dr}\right) = 2\pi q_o \,. \tag{1}$$

The boundary conditions are

$$T(R_o) = T_b \,, \quad \left(2\pi k r\frac{dT}{dr}\right)_{r=0} = 0 \,. \tag{2}$$

The exact solution of the problem can be obtained by integrating Eq. (1) and evaluating the constants of the integration with the help of the boundary conditions in Eq. (2):

$$T(r) = \frac{q_o R_o^2}{4k}\left[1 - \left(\frac{r}{R_o}\right)^2\right] + T_b . \tag{3}$$

If we define the dimensionless temperature T^* as:

$$T^* \equiv \frac{k(T - T_b)}{q_o R_o^2} , \tag{4}$$

the dimensionless temperature T^* at the center of the cylinder according to the exact solution from Eq. (3) is 0.2500, whereas the FEM solution [1] is 0.3333, 0.2778, 0.2587, and 0.2526 according to the one-, two-, four-, and eight-element models, respectively.

The finite element solutions obtained using one-, two-, four-, and eight-element meshes of the linear elements are compared with the exact solution in Table 1, which shows the convergence of the finite element solutions to the exact solution with an increasing number of elements. Therefore, FEM analyses will produce more accurate solutions when the mesh interval is decreased.

3. IMPLEMENTATION OF THE FVM INTO THE CATHENA CODE

The FVM is applied to the CATHENA wall conduction model to avoid the mesh size effect on the fuel temperature prediction. For this purpose the numerical scheme using the FVM for the CATHENA radial conduction model is developed and implemented into the CATHENA code. Here we are to develop the FVM based on the control volume integration [3] for the heat conduction in the cylindrical geometry. The integral form of the heat conduction equation is:

$$\iiint_V C_\rho(T,r)\frac{\partial T}{\partial t}(r,t)\,dV = \iint_A k(T,r)\nabla T(r,t)\cdot dA + \iiint_V S(r,t)\,dV , \tag{5}$$

where

k	=	thermal conductivity (W m^{-1}K^{-1})
A	=	surface area (m^2)
S	=	internal heat source (W m^{-3})
t	=	time (sec)
T	=	temperature (K)
V	=	volume (m^3)
r	=	radius in the cylindrical coordinates (m)
C_ρ	=	volumetric heat capacity (J m^{-3}K^{-1}).

Figure 2 shows the typical mesh points for the finite volume method. The subscripts are space indexes indicating the mesh point number. The δr 's indicate mesh point spaces. Between the mesh points (in the mesh element), the thermal properties, k and C_ρ, and the source term, S are assumed spatially constant.

The key point of the FVM is the integration of the governing equation over a control volume to yield a discretised equation at its nodal point 'e'.

Using a forward difference for the time derivative, the first term of Eq. (5) for the typical control volume in Figure 2 is approximated by

$$\iiint_V C_\rho(T,r)\frac{\partial T}{\partial t}(r,t)\,dV$$

$$\approx \left[C_{\rho,e-1}\times\pi\delta r_{e-1}(r_e-0.25\,\delta r_{e-1})+C_{\rho,e}\times\pi\delta r_e(r_e+0.25\,\delta r_e)\right]\frac{\left(T_e^{n+1}-T_e^n\right)}{\Delta t}, \tag{6}$$

where the superscript n refers to time; thus, T_e^n indicates the temperature at mesh point 'e' at time t^n, and T_e^{n+1} indicates the temperature at mesh point 'e' at time $t^{n+1}=t^n+\Delta t$.

The diffusion term of Eq. (5) for the surface of typical control volume is approximated by

$$\iint_A k(T,r)\nabla T(r,t)\cdot dA$$

$$\approx (1-w)\left\{\left[k_{e-1}\times 2\pi\left(r_e-0.5\,\delta r_{e-1}\right)\right]\frac{\left(T_{e-1}^n-T_e^n\right)}{\delta r_{e-1}}+\left[k_e\times 2\pi\left(r_e+0.5\,\delta r_e\right)\right]\frac{\left(T_{e+1}^n-T_e^n\right)}{\delta r_e}\right\}$$
$$+w\left\{\left[k_{e-1}\times 2\pi\left(r_e-0.5\,\delta r_{e-1}\right)\right]\frac{\left(T_{e-1}^{n+1}-T_e^{n+1}\right)}{\delta r_{e-1}}+\left[k_e\times 2\pi\left(r_e+0.5\,\delta r_e\right)\right]\frac{\left(T_{e+1}^{n+1}-T_e^{n+1}\right)}{\delta r_e}\right\}, \tag{7}$$

where the implicit formulation with $w=0.5$ is used, which is called the Crank-Nicolson method [4].

The source term of Eq. (5) is approximated as

$$\iiint_V S(r,t)dV \approx S_{e-1}\times\pi\delta r_{e-1}(r_e-0.25\,\delta r_{e-1})+S_e\times\pi\delta r_e(r_e+0.25\,\delta r_e). \tag{8}$$

Using the Equations (6), (7), and (8), the general discretized equations for the e-th interior mesh point ($e=2,3,\ldots,E-1,E$) can be arranged as

$$a_e\,T_{e-1}^{n+1}+b_e\,T_e^{n+1}+c_e\,T_{e+1}^{n+1}=d_e, \tag{9}$$

where

$$a_e=-\pi\,k_{e-1}(r_e-0.5\,\delta r_{e-1})\,\Delta t\,/\,\delta r_{e-1}, \tag{10}$$

$$b_e = \left[C_{\rho,e-1} \times \pi \delta r_{e-1}(r_e - 0.25\,\delta r_{e-1}) + C_{\rho,e} \times \pi \delta r_e (r_e + 0.25\,\delta r_e)\right] - a_e - c_e, \tag{11}$$

$$c_e = -\pi\, k_e (r_e + 0.5\,\delta r_e)\,\Delta t / \delta r_e, \tag{12}$$

$$\begin{aligned} d_e = {} & -a_e\, T_{e-1}^n + [b_e + 2(a_e + c_e)] T_e^n - c_e\, T_{e+1}^n \\ & + \Delta t [S_{e-1} \times \pi \delta r_{e-1}(r_e - 0.25\,\delta r_{e-1}) + S_e \times \pi \delta r_e (r_e + 0.25\,\delta r_e)]. \end{aligned} \tag{13}$$

For the control volumes that are adjacent to the boundaries the general discretized equations in Eq. (9) are modified to incorporate the boundary conditions.

Since the left boundary condition (at $r_1 = 0$) of Eq. (5) is normally the symmetry boundary condition (BC), the discretised equation for the left boundary is

$$b_1\, T_1^{n+1} + c_1\, T_2^{n+1} = d_1 \quad \text{with BC: } -k_1 \left.\frac{\partial T}{\partial r}\right|_{r=r_1} = 0, \tag{14}$$

where

$$b_1 = C_{\rho,1} \times 0.25\pi\,\delta r_1^2 - c_1, \tag{15}$$

$$c_1 = -0.5\pi\, k_1\, \Delta t, \tag{16}$$

$$d_1 = (b_1 + 2c_1) T_1^n - c_1\, T_2^n + \Delta t (S_1 \times 0.25\pi\,\delta r_1^2). \tag{17}$$

If the desired right boundary condition (at $r_{E+1} = R_o$) is that the heat transferred out of the surface equals a heat transfer coefficient (h_c) times the difference between the surface temperature (T_{E+1}) and the sink temperature (T_f), i.e.,

$$-k_E \left.\frac{\partial T}{\partial r}\right|_{r=r_{E+1}} = h_c (T_{E+1} - T_f), \tag{18}$$

then, the discretised equation for the right boundary is

$$a_{E+1}\, T_E^{n+1} + b_{E+1}\, T_{E+1}^{n+1} = d_{E+1}, \tag{19}$$

where

$$a_{E+1} = -\pi\, k_E (r_{E+1} - 0.5\,\delta r_E)\,\Delta t / \delta r_E, \tag{20}$$

$$b_{E+1} = C_{\rho,E} \times \pi \delta r_E (r_{E+1} - 0.25\,\delta r_E) + 2\pi r_{E+1}\, h_c\, \Delta t - a_{E+1}, \tag{21}$$

$$\begin{aligned} d_{E+1} = {} & -a_{E+1}\, T_E^n + (b_{E+1} + 2a_{E+1} - 2\pi r_{E+1}\, h_c\, \Delta t) T_{E+1}^n \\ & + 2\pi r_{E+1} h_c T_f\, \Delta t + \Delta t [S_E \times \pi \delta r_E (r_{E+1} - 0.25\,\delta r_E)]. \end{aligned} \tag{22}$$

The discretized equations for the mesh points, 'e' [Equations (9), (14), and (19)] lead to a tri-diagonal set of $E+1$ equations:

$$\begin{bmatrix} b_1 & c_1 & & & & \\ a_2 & b_2 & c_2 & & & \\ & \cdots & \cdots & & & \\ & & \cdots & \cdots & \cdots & \\ & & & a_E & b_E & c_E \\ & & & & a_{E+1} & b_{E+1} \end{bmatrix} \begin{bmatrix} T_1^{n+1} \\ T_2^{n+1} \\ \cdots \\ \cdots \\ T_E^{n+1} \\ T_{E+1}^{n+1} \end{bmatrix} = \begin{bmatrix} d_1 \\ d_2 \\ \cdots \\ \cdots \\ d_E \\ d_{E+1} \end{bmatrix}. \tag{23}$$

In the subroutine "walr.f" of the original CATHENA version the radial conduction equations by the FEM are solved to obtain T_e^{n+1}, while the matrix in Eq. (23) is solved in the CATHENA with the FVM.

4. COMPARISON OF FEM AND FVM MODELS IN CATHENA CODE

The accuracy and validity of the finite volume model in the CATHENA code are tested by one-dimensional steady state and transient heat conduction problems in a cylindrical geometry, for which the exact solutions are available.

4.1 Steady State Problem

The first problem concerns the stationary heat conduction and is governed by Eq. (1), with a constant thermal conductivity k, and heat source q_o. The geometry and boundary conditions are shown in Fig. 1, and the exact solution is given in Eq. (3). A constant temperature on the boundary surface and a uniform internal heat generation rate are assumed for the steady state problem.

Figures 3 and 4 show the calculation results by the CATHENA with the FEM and the FVM, respectively. The mesh size effect on the temperature prediction is clear in Fig. 3 as expected in section 2. However, the temperature distribution by the CATHENA with the FVM is found to give the same analytical solutions and consistent results with varying mesh sizes. Therefore, if the positions of the nodal points are the same, there is no difference in the temperature predictions between the coarse and the fine mesh schemes, which depends on the user choice.

4.2 Transient Problem

We now extend the test problem of heat conduction to include time dependent behaviour.

In the transient heat conduction problem, a cylinder is initially at a uniform temperature (T_i) and suddenly; its boundary surface ($r = R_o$) is subjected to convection with a constant heat transfer coefficient (h_c) into an ambient at a constant temperature (T_∞). The temperature distribution for this situation can be calculated, and the results presented in the form of transient-temperature charts [5] using various dimensionless quantities defined as:

$$Bi = \frac{h_c R_o}{k} = \text{Biot number,} \tag{24}$$

$$\tau = \frac{\alpha t}{R_o^2} = \text{dimensionless time (Fourier number),} \tag{25}$$

$$\theta = \frac{T(r,t) - T_\infty}{T_i - T_\infty} = \text{dimensionless temperature,} \tag{26}$$

The results for the center temperature $\theta(0,\tau)$ are shown by solid lines in the temperature chart (T-chart) in Fig. 5 as a function of the dimensionless time τ for several different values of the parameter $1/Bi$. In addition the CATHENA predictions with the FEM (original version) and the FVM are compared with the values from T-chart in Fig.5. The geometry and boundary conditions for adjusting the values of the parameter $1/Bi$, are shown in Table 2.

It is shown that the CATHENA with the FVM as well as that with the previous FEM method shows the same time-dependent temperature behaviour as that given by the solutions of dimensionless heat conduction equation for a long cylinder. However, the FEM method initially shows a higher temperature prediction than the initial value even though the cylinder is cooled by the boundary condition (Figure 6).

5. CONCLUSIONS

The numerical scheme for a radial conduction model of the CATHENA code is replaced with FVM to remove the mesh size effect on the fuel temperature prediction. For this purpose the following works were conducted in the present study.

- The FEM solutions for the radial heat conduction in the cylindrical geometry with a different number of elements in the mesh scheme were compared with the exact solution, which showed the convergence of the finite element solutions to the exact solution with an increasing number of elements.
- The numerical scheme using the FVM for the CATHENA radial conduction model was developed and implemented in the CATHENA code. From the integration of the governing equation over a control volume the discretised equations at its nodal point are derived and arranged in the matrix form, which should be solved in the CATHENA with the FVM. A forward difference scheme was used for the time derivative and the Crank-Nicolson method was used for the diffusion term of the governing equation.
- The accuracy and validity of the finite volume model in the CATHENA code were tested by one-dimensional steady state and transient heat conduction problems in the cylindrical geometry, for which the exact solutions are available. The steady state solutions by the FVM model were found to give the same results as the analytical solutions and consistent results with varying mesh sizes, while the original CATHENA with the FEM over-predicts the center temperature with larger mesh sizes. The new model also closely follows the analytical solutions of the dimensionless heat conduction equation for a long cylinder.

REFERENCES

1. J.N. Reddy, "An Introduction to the Finite Element Method", International Editions, McGraw-Hill (1993).
2. T.G. Beuthe, and B.N. Hanna (editors), "CATHENA MOD-3.5c/Rev 0 Theoretical Manual", CANDU Owners Group Report, COG-99-007 (1999).
3. H.K. Versteeg and W. Malalasekera, "An Introduction to Computational Fluid Dynamics: The Finite Volume Method", Longman (1995).
4. Klaus A. Hoffmann, "Computational Fluid Dynamics for Engineers", Engineering Education System™, Austin USA (1989).
5. M. Necati Özişik, "Heat Transfer: A Basic Approach", McGraw-Hill (1985).

Table 1. Comparison of the finite element and exact solutions for heat transfer in a radially symmetric cylinder

$\frac{r}{R_o}$	$T^* \equiv \frac{k(T-T_b)}{q_o R_o^2}$				
	One-element	Two-element	Four-element	Eight-element	Exact
0.000	0.3333	0.2778	0.2587	0.2526	0.2500
0.125				0.2474	0.2461
0.250			0.2379	0.2353	0.2344
0.375				0.2155	0.2148
0.500		0.1944	0.1893	0.1880	0.1875
0.625				0.1526	0.1523
0.750			0.1101	0.1096	0.1094
0.875				0.0587	0.0586
1.000	0.0000	0.0000	0.0000	0.0000	0.0000

Table 2. Boundary conditions for the Transient Conduction Problem

$1/Bi$	$R_o\,(mm)$	$k\,(W/m$□$K)$	$\alpha\,(\times 10^6\,m^2/s)$	T_i (°C)	T_∞ (°C)	$h_c\,(W/m^2$□$K)$
0.0	6.1	3.0	0.909	1000.0	435.7	10^7
0.1						4918
0.2						2459

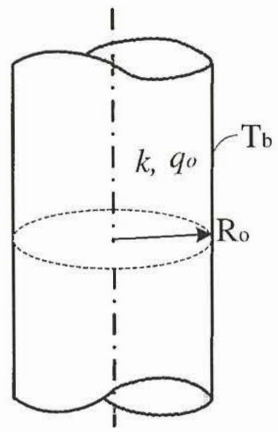

Fig. 1. Configuration of radial heat conduction in cylinder

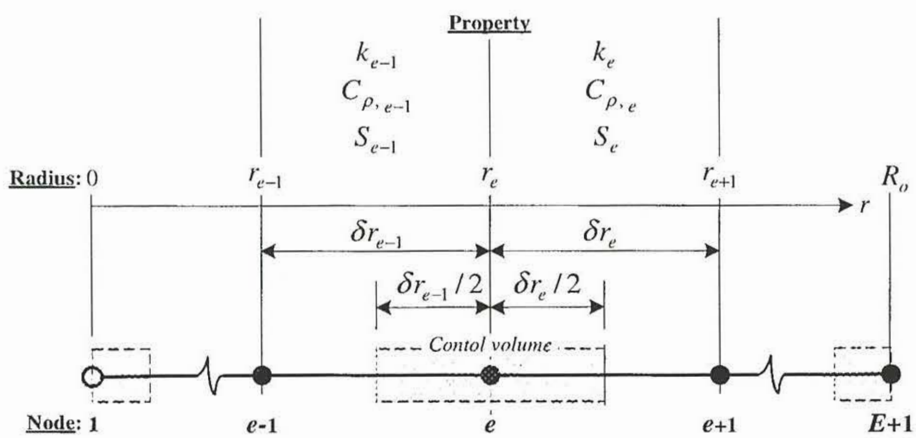

Fig. 2. The mesh points for FVM

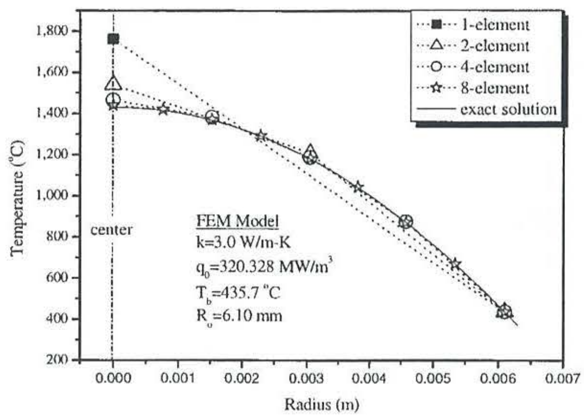

Fig. 3. Temperature distributions for steady state problem by CATHENA with FEM

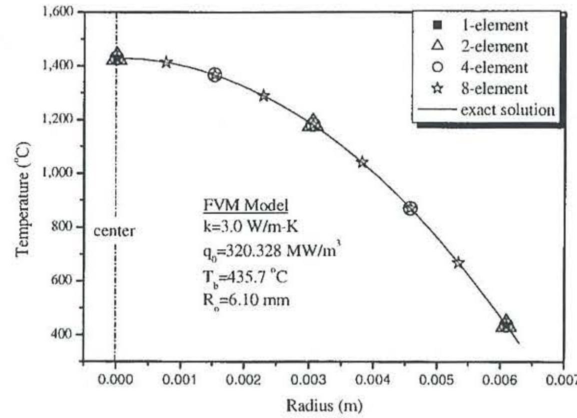

Fig. 4. Temperature distributions for steady state problem by CATHENA with FVM

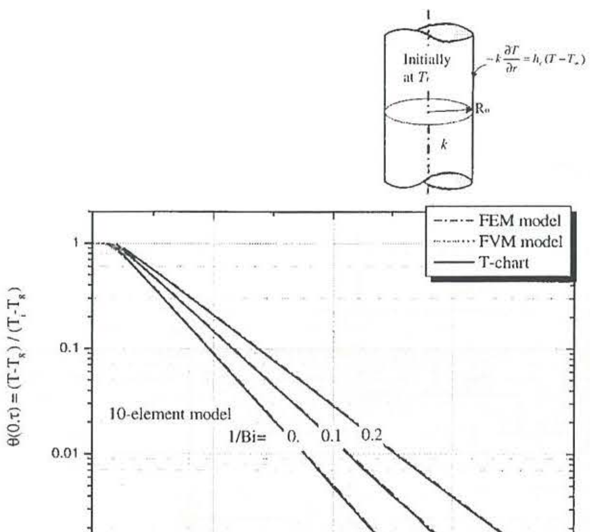

Fig. 5. Temperature predictions for transient problem

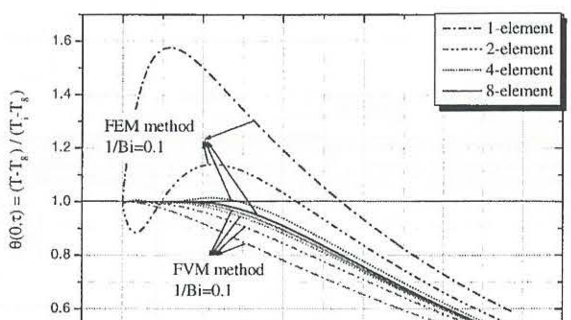

Fig. 6. The transient responses from the initial value both by FEM and FVM methods